PERIODICA POLYTECHNICA SER. EL. ENG. VOL. 39, NO. 2, PP. 167-178 (1995)

PROCESSING OF SLAR IMAGES

György G. VASS, Attila ZÓLOMY and László KALMÁR

Department of Microwave Telecommunications
Technical University of Budapest
H-1521 Budapest, Hungary
Fax: (+36-1) 463 3289
E-mail: d-vass@nov.mht.bme.hu
Phone of Gy. Vass: (+36-1) 463 1559

Received: Sept. 20, 1995

Abstract

An X-band Side Looking Airborne Radar (SLAR) has been developed and constructed. The recorded raw images had to be corrected both radiometrically and geometrically. To achieve this goal, different digital image processing methods have been applied. The obtained results are images fitting well to the original maps of the landscapes. Final resolution of the corrected images is 10...15 m.

Keywords: microwave remote sensing, radar, image processing.

1. Introduction

Airborne and spaceborne imaging radars collect large amounts of useful data from almost all regions of the Earth. The first imaging radars were used during World War II, when microwave technology was developed.

Microwave radar can obtain images at any time of day and night. In addition, microwaves can easily penetrate clouds since atmospheric attenuation is relatively low in this frequency range. This all-weather capability is one of the main advantages of imaging radars in relation to the conventional optical sensors. Radars development was classified during the War and for that reason codes were attributed to the wavelength used, such as L-band, C-band or X-band. After World War II, Side Looking Airborne Radars (SLAR) were developed for terrain surveillance. In this case, the radar illuminates a strip of terrain parallel to the flight path (see *Fig. 1*). Backscattered signals were recorded on a film using a CRT. Recently, digital image forming methods have gained increased popularity (PÉTER et al., 1994). This paper describes basic image forming methods of the SLAR and the subsequent corrections needed.

2. Image Forming of the SLAR

The SLAR is an active remote sensing system which can create the microwave photograph of the ground surface (cf. MOORE, 1975). Its operation is based on the principle that emitted narrow microwave pulses return in the receiver with considerable time delay from ground points being at different distances from the radar. Power of the reflected signal is proportional to the magnitude of the reflection cross-section and inversely proportional to the fourth power of the distance. These dependencies are usually represented by the radar equation (1.1).

$$P_r = \frac{P_t G_0^2 \lambda^2}{(4\pi)^3 R^4} \sigma, \tag{1.1}$$

where

P_r	received power [W]
P_t	transmitted power [W]
G_0	antenna gain
λ	wavelength [m]
R	slant range [m] (from the radar to the ground)
σ	backscattering coefficient [m^2]

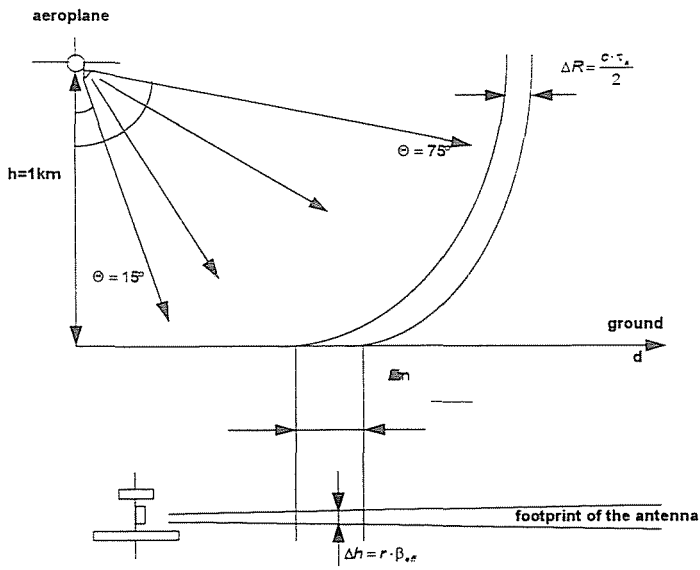

Fig. 1. Operation of the SLAR

As it will be shown, the flight altitude is a crucial factor in terms of different corrections of the recorded images. A typical value is 1 km, however, it can

considerably vary even during a single flight depending on the atmospheric conditions. The altitude can be calculated in a straightforward way by counting the time elapsed until the first return:

$$t_{\min} = \frac{2h}{c}, \tag{1.2}$$

where h denotes the flight altitude and c is the velocity of light. An altitude of 1 km corresponds to a $t_{\min}$ of 6...7 μs. Impulses from further apart arrive later in time. Recording of the time series of the reflected pulses allows to obtain a reflection graph of a particular strip of terrain. This, in reality, forms one single row of the remotely sensed image. As signals arriving from longer distances do not exceed the sensitivity threshold of the receiver unit, they are not recorded. These signals, actually, arrive from a direction close to horizontal. In addition, small incidence angles at these parts of the terrain cause decrease in backscattering coefficient, thus, weaker returns. Consequently, it is reasonable to introduce an upper limit for the time interval of the reception and ignore all the returns later. This time limit can be defined as follows:

$$t_{\max} = \frac{2h}{\cos\Theta_{\max}}\frac{1}{c}, \tag{1.3}$$

where $\Theta_{\max}$ is the incident angle corresponding to the last recorded pixel. It has the value of approximately 75°. A typical value of $t_{\max}$ is 30...40 μs. On the other hand, reflections from the close vicinity of the aircraft show up usually extremely low time differences, thus, a significant degradation of across track resolution can be observed in this region. As a conclusion, a reasonable choice of the observation angle is ca. Θ=15 ..75°.

Resolution is one of the main characteristic features of microwave imaging. Resolution range of the SLAR is mainly determined by the duration of the emitted pulses (50 ns, in our case). In addition, ground range resolution also varies with the incident angle (which is a function of distance) and can be formulated as follows:

$$\Delta m = \frac{\tau_{tr} c}{2\sin\Theta}, \tag{1.4}$$

where τ_{tr} is the length of the emitted pulse and Θ is the local incident angle. A typical value of Δm is in the range of 7.5 m...10 m. Resolution in the azimuth direction (or along-track resolution), on the other hand, is basically determined by the width of the antenna main lobe (β_{eff} = 0.01 rad). Typical value is 10 m...15 m. One of the most serious sources

of error in microwave imaging is the presence of speckle noise. In order to overcome this failure it is common to apply an appropriate averaging procedure. Since the speckle noise can be considered as a random, uncorrelated process, it can be assumed with a great certainty that its magnitude will be reduced during the averaging procedure. It is worth mentioning that the transmitter emits pulses in a millisecond rate in order to assure a certain level of emission efficiency of its magnetron. On the other hand, we receive only every twentieth return. This constraint has, however, no significant influence on the quality of our images. In the way described above, scattering coefficients from different points of the surface can be obtained, and from these data first a single row and in turn a complete image can be created.

Construction of the SLAR is shown in *Fig. 2* with the Radar Unit displayed more detailed in *Fig. 3* (MIHÁLY et al., 1985). Signals arriving at the antenna are first converted down in the Radar Unit to a suitable intermediate frequency, IF (60 MHz in our case). An onboard Automatic Gain Control (AGC) unit has the duty to adapt the actual received power to the sensitivity of the receiver by adjusting an appropriate gain in the IF amplifier stage. This unit assures a constant average signal level in the receiver, however, rapid changes within rows are ignored. The Sensitivity Time Control (STC) unit adjusts the signal level also within a single row, thus, it can partly compensate for the unwanted effect of the antenna pattern and other unpleasant symptoms. We note here that, furthermore, sophisticated radiometric corrections will be necessary to eliminate all the defects in detail. They will be discussed later in this paper. The compensated signal is demodulated and sampled with a 20 MHz rate. The 8 bit converted digital signal is downloaded into an appropriate buffer from which it will be transferred into the operational memory of the PC. This data transfer occurs between reception of two adjacent rows. Finally, display of the row on the screen is performed. *Table 1* summarizes the main system parameters of the SLAR.

3. Radiometric Correction

Radar images should represent microwave scattering properties of the ground surface, an information carried by the backscattering coefficient. In an ideal case, the received power in the radar is a direct function of the backscattering coefficient. However, looking at (1.1) we can see that there are many other determining factors as well, which have to be compensated for in order to get the desired result. Influences can be classified into the following categories:

Table 1
SLAR System Parameters

Operating frequency	9.4 GHz (X-band)
Transmitted power	3.5 kW
Transmitted pulse-width	50 ns
Polarization	VV
Receiver bandwidth	16 MHz
Receiver sensitivity	−90 dBm
Antenna beamwidth	0.01 rad (0.6 deg)
PRF	50 Hz
Sampling rate/depth	20 MHz / 8 bit
Integrated samples per pixel	8

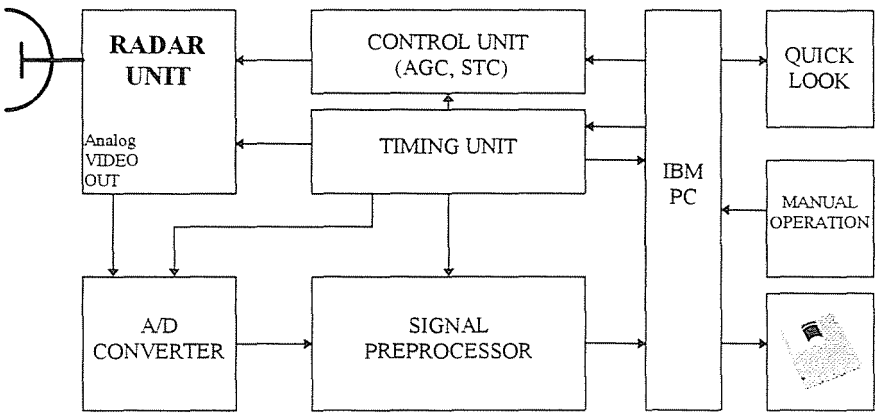

Fig. 2. Schematic diagram of the SLAR

- effect of the varying radar–target distance;
- effects of the antenna pattern;
- the radar backscatter as a function of local incidence angle.

Round-trip path loss increases with the fourth power of range, which causes signals arriving from further points on the ground to be much weaker than those coming from close terrain points. As a consequence, brightness within a single row of the images has a strong decay towards the end (see *Fig. 5*). This function is, however, an explicit one, and can be easily modeled mathematically.

The antenna has a fan-beam and, thus, its gain is a function of elevation and azimuth. The gain function of the antenna mounted under an aircraft may differ from the gain function of the antenna in free space because of the presence of obstacles in the near field of the antenna. The

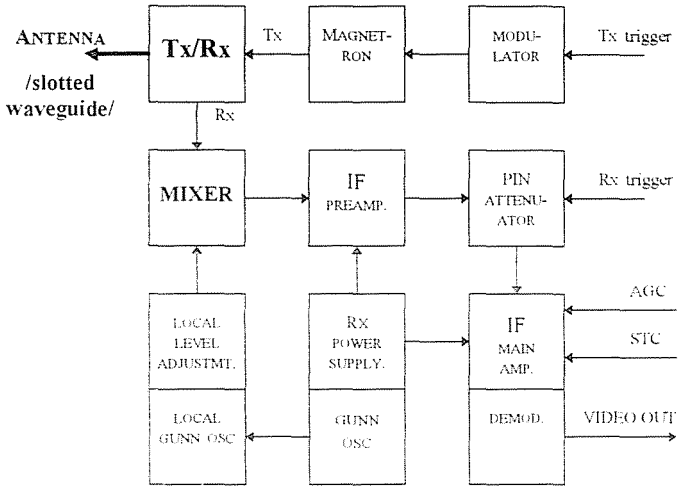

Fig. 3. The radar unit

strongest effect has, among all these obstacles, the wing surface, from which the radar waves can almost perfectly reflect. The complex sum of the direct and reflected waves results in an interference in the receiver which, in turn, adversely affects the quality of the images. This phenomenon can be observed as dark and bright stripes in the images parallel to the flight direction (see *Fig. 5* and *Fig. 6*). In order to eliminate the effect of the antenna pattern, together with the effect of the range dependence of the signal, a suitable model has been established. First, the nominal antenna pattern in a vertical plane has been modified in such a way that it includes the mentioned range dependence, too. The smooth curve of *Fig. 4* illustrates this function in a polar system of coordinate axes. The applied modification has the virtual effect as if the antenna shifted towards the ground by ca. 5 degrees. In a second stage of modeling, also the effect of the wing surface has been taken into account. In this model, the wing has been substituted by an infinite, ideally conducting metal surface mounted above the antenna, which proved to be a good approximation of the real situation. The calculated result is the rapidly changing curve of *Fig. 4*, superimposed on the original. The curve at the lower edge of *Fig. 4* shows how a single row of the final image will be influenced by these effects. Comparisons of the calculated results with the graph of particular rows in the recorded images led to surprisingly good coincidences, which also demonstrated the truth of our hypothetical model.

A third influence comes from the fact that the ground surface with all the different objects on it has usually different backscattering properties in the different directions. Since the local incidence angle of the emitted

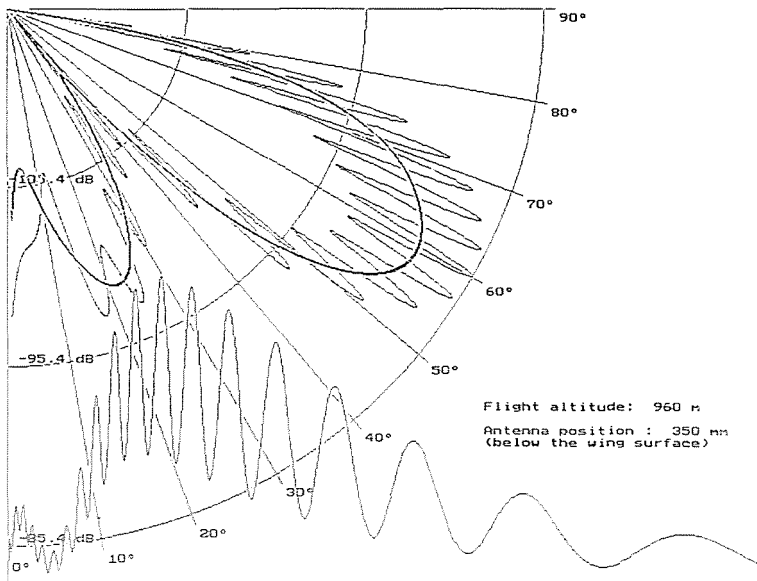

Fig. 4. Modeling the effects of the antenna pattern. Reflections from the wing surface may cause severe interference

waves varies with distance, even in an ideal case with homogeneous terrain, we could observe variations in the received signal. The backscattering coefficient as a function of incidence angle is, in fact, determined by numerous parameters of the object (like shape, altitude, surface quality, etc.), and thus, it is quite often modeled statistically. Since this effect is presumably minor, compared to the former ones, we did not include it into our model.

There are two major ways how to correct radiometric distortions of the recordings: one which modifies received signal levels directly during acquisition but before image forming; and another one which manipulates the final image by modifying individual pixel values and applying different digital image processing techniques. The former method takes place onboard the airplane, while the latter one is usually performed in suitable computer environment after landing. Each method has its advantage: digital image processing is a comfortable and highly effective tool to correct different failures, however, since it works on the final, digitized image, it is unable to enhance radiometric resolution. This is especially disagreeable when the image contains dark regions (as a consequence of weak received signals).

The Sensitivity Time Control STC has already been mentioned in this paper (see Section 2). It compensates for most of the range dependence

of the radar signal, as it simply raises the sensitivity of the receiver when reception of weak returns occurs. In favor of an increased system flexibility, we carried out some experiments to let the sensitivity – time function to be modified by the user and adapted more to the actual conditions. In these experiments we used a row of potentiometers to adjust the desired function manually.

Beyond all the different methods mentioned here, the ultimate solution to eliminate unwanted radiometric distortions is a perfect system calibration, which requires a test flight over a relatively smooth, homogeneous terrain. By averaging all the rows of such a recording, an optimal correction function can be well approximated. Corner reflectors can be useful for a quantitative calibration of the system.

4. Geometric Correction

Raw images created by the SLAR are usually corrupted by severe geometrical distortions. Geometrical correction is a procedure of eliminating these unwanted effects by changing positions of individual pixels, as opposed to radiometric corrections – treated in the previous part – where only pixel values have been changed. Final goal is to get geographically correct images which can be easily registered to real topographic maps by applying simple linear scaling operations. There are several sources of error which can cause geometric distortions. Main categories are the following:

- the side-looking principle of the radar;
- aircraft movement irregularities (roll, pitch, yaw, unstable velocity);
- layover, shadowing, foreshortening.

Imaging radars usually operate in a side-looking configuration, which allows the returns representing the microwave backscattering properties of the imaged terrain to well separate in time. On the other hand, this configuration has the drawback that adjacent pixels of the images will not correspond to equal distances on the ground and, as a consequence, resolution will not be unique within rows. Especially at the parts of the terrain close to the aircraft, resolution can significantly decline (see e. g. along the left edge of *Fig. 6*). This type of distortions can be, however, easily corrected in that the whole image is resampled according to a unique range scale on the ground (such images can be seen in *Fig. 5* and *Fig. 7*). Resampling is performed by the use of a suitable interpolation method (e. g. cubic spline interpolation). The required formula for the slant range to ground range transformation can be easily obtained knowing the exact flight altitude and applying the Pythagorean theorem. The flight altitude is

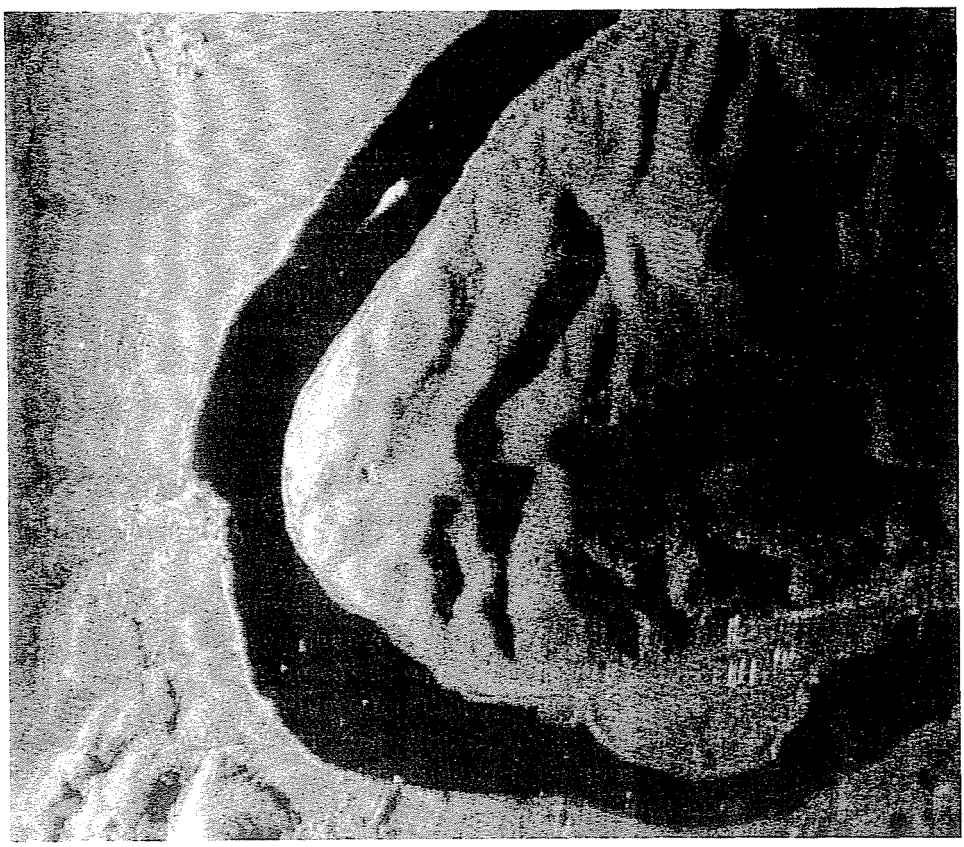

Fig. 5.

usually estimated by measuring the time between the emission of the pulses and their first ground return, and calculating the corresponding distance. The second group of defects, caused by the irregular movement of the aircraft, consists of less deterministic features. In the radar image of *Fig. 5*, for instance, a random shift of the dark and bright interference stripes can be clearly observed. This is a consequence of aircraft roll. Aircraft yaw and pitch generally also cause distortions. Most serious defects are pixel misregistration and a decrease in azimuth resolution. These kinds of distortions are usually difficult to compensate for, since correction requires exact knowledge of certain aircraft parameters (e.g. geographical co-ordinates, flight velocity, altitude). In addition, all these data should be recorded together with the image data, simultaneously. A perfect synchro-

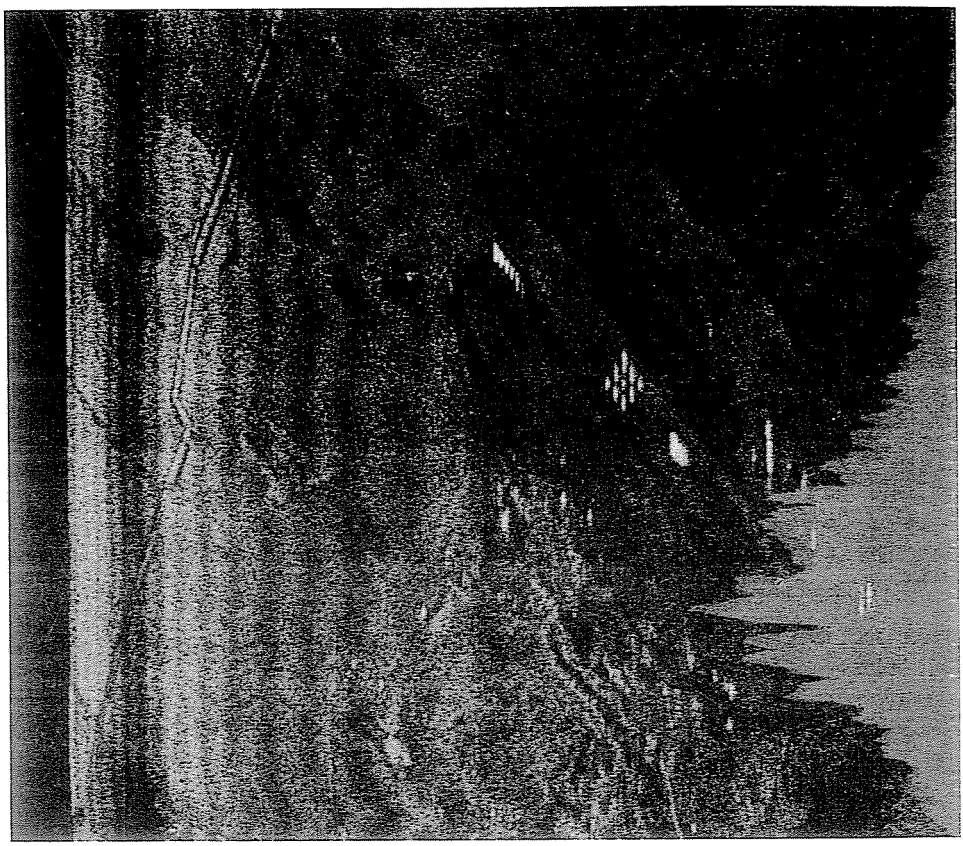

Fig. 6.

the flight and image data is inevitable to achieve a satisfactory correction. As a summary, owing to the lack of precise flight parameters, our airborne system failed to allow the correction of distortions caused by aircraft movements. Encouraging results have been reported, however, by other authors about airborne radar experiments. The aircraft has been equipped with modern navigation aids, thus, motion parameters have been available for the correction. Majority of the geometric distortions caused by the aircraft could be eliminated to a satisfactory extent (HOOGEBOOM et al., 1983, 1984).

In addition to the mentioned geometrical distortions – for which correction methods have been available as a partial elimination – there are also some geometrical defects in the microwave images, for which compen-

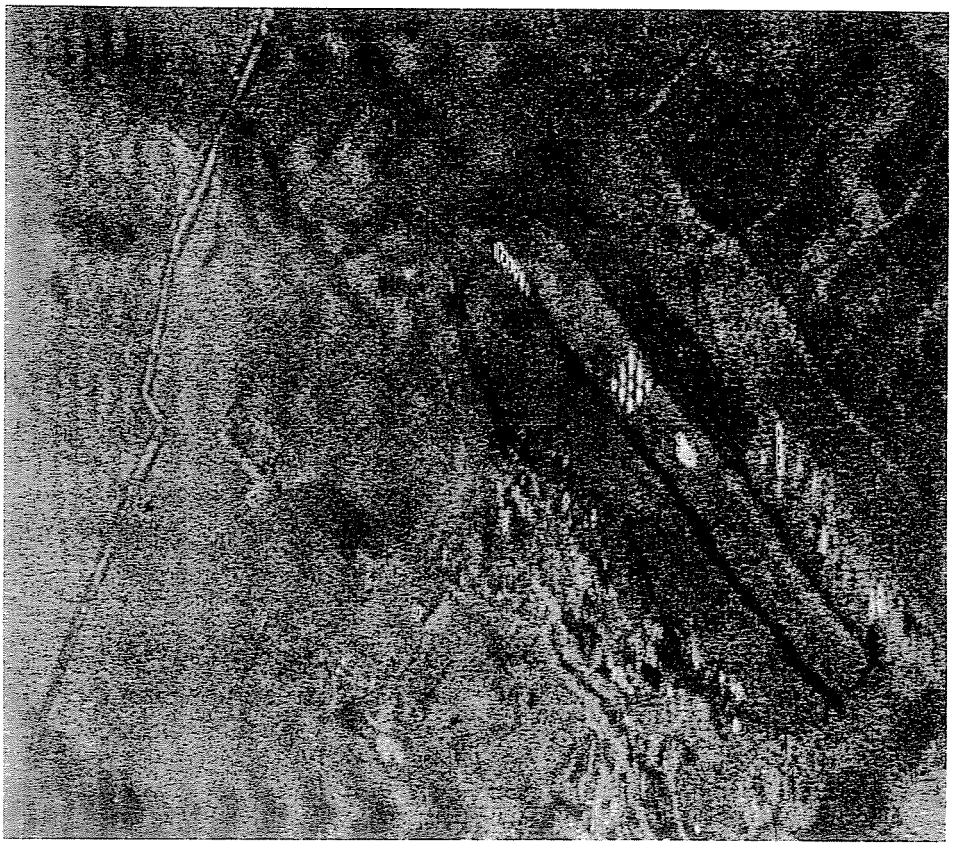

Fig. 7.

sation requires exact knowledge of the imaged terrain or, in some cases, it is even theoretically impossible. Most of these errors are caused by extreme variations in terrain elevation. A relatively high mountain can have large *shadows* in the microwave image (see *Fig. 5*), as a consequence of the oblique illumination (side-looking principle). Information will be lost in these poorly illuminated regions, which cannot be recovered by subsequent corrections. Furthermore, note that the side of the mountain illuminated by the radar will appear shorter in the image than its real size, since radar waves return earlier from elevated points than from the ground. This phenomenon, called foreshortening, can be theoretically compensated for if a digital elevation map (DEM) of the imaged terrain is available. In extreme cases, radar waves arriving from elevated points can even precede reflec-

tions from the ground. This causes undesirable layover in the corresponding part of image. Since separation of the signals arriving from different terrain parts is impossible, layover generally cannot be corrected.

5. Conclusion

Side Looking Airborne Radar (SLAR) is a cost-effective and powerful solution for obtaining microwave images from relatively small land regions with reasonable resolution. Acquisition can be performed day and night, irrespective of the actual meteorological conditions. The low flight altitudes – compared to modern spaceborne sensors – (approx. 1 km) have the consequence that special attention has to be paid to compensation for the distortions present in the recorded images. Majority of these defects are caused by the side-looking principle of the radar, and the irregular movement of the aircraft (as a consequence of atmospheric disturbances). In this study different correction methods have been tested and evaluated. *Fig. 7* shows a geometrically as well as radiometrically corrected image. (Original raw image is shown in *Fig. 6*).

Results have shown that most of the unwanted distortions of the radar images can be eliminated successfully by the use of appropriate correction algorithms. Suggestions for the improvement of these algorithms (e. g. by the involvement of aircraft parameters) have also been made.

Acknowledgement

The authors would like to express their thanks to Mr. Farkas and Mr. Seller, supervisors of the development, for their useful advices and constant encouragement.

References

HOOGEBOOM, P. – BINNENKADE, P. – VEUGEN, L. M. M. (1984): An Algorithm for Radiometric and Geometric Correction of Digital SLAR Data. *IEEE Trans. on Geosci. and Remote Sensing*, Vol. GE-22, No. 6, pp. 570–576.

HOOGEBOOM, P. (1983): Preprocessing of Side-looking Airborne Radar Data. *Int. Journal on Remote Sensing*, Vol. 4, No. 3, pp. 631–637.

MIHÁLY, S. – SELLER, R. – FARKAS, B. – GÖDÖR, É. – BOZSÓKI, I. (1985): X-band Active Microwave Backscattering and Imaging Experiments in Hungary. Report of the Dept. of Microwave Telecommunications, Technical Univ. of Budapest.

MOORE, R. K. (1975): An Inexpensive Side Looking Radar with a Novel Display. *Proc. of IEEE International Radar Conference*, pp. 552–526.

PÉTER, Z. – ZÓLOMY, A. – KALMÁR, L. – VASS, GY. (1994): Radarképek készitése és feldolgozása (Acquisition and Processing of Radar Imagery; in Hungarian). *Scientific Student Conference 1994*, Technical Univ. of Budapest.